Proc. Natl. Acad. Sci. USA
Vol. 86, pp. 1515–1518, March 1989
Biophysics

Why are blue visual pigments blue? A resonance Raman microprobe study

(opsin shift/color vision/rhodopsin/wavelength regulation/vibrational spectroscopy)

GLEN R. LOPPNOW, BRIDGETTE A. BARRY*, AND RICHARD A. MATHIES†

Department of Chemistry, University of California, Berkeley, CA 94720

Communicated by Lubert Stryer, November 21, 1988 (received for review October 27, 1988)

ABSTRACT **A resonance Raman microscope has been developed to study the structure of the retinal prosthetic group in the visual pigments of individual photoreceptor cells. Raman vibrational spectra are obtained by focusing the probe laser on intact photoreceptors frozen on a 77 K cold stage. To elucidate the mechanism of wavelength regulation in blue visual pigments, we have used this apparatus to study the structure of the chromophore in the 440-nm absorbing pigment found in "green rods" of the toad (*Bufo marinus*). The 9-*cis* isorhodopsin form of the green rod pigment exhibits a 1662-cm^{-1} C=NH^+ Schiff base stretching mode that shifts to 1636 cm^{-1} in deuterium-substituted H_2O. This demonstrates that the Schiff base linkage to the protein is protonated. Protonation of the Schiff base is sufficient to explain the 440-nm absorption maximum of this pigment without invoking any additional protein–chromophore interactions. The absence of additional perturbations is supported by the observation that the ethylenic band and the perturbation-sensitive C-10–C-11 and C-14–C-15 stretching modes have the same frequency as those of the 9-*cis* protonated retinal Schiff base in solution. Our demonstration that a blue visual pigment contains an *unperturbed protonated* Schiff base provides experimental evidence that the protein charge perturbation responsible for the opsin shift in the 500-nm absorbing pigments is removed in the opsins of blue pigments, as suggested by the sequence data.**

Vertebrate visual pigments contain an 11-*cis* retinal chromophore (structure **1**) bound via a Schiff base linkage to a specific lysine of the 41,000-dalton apoprotein, opsin. Upon

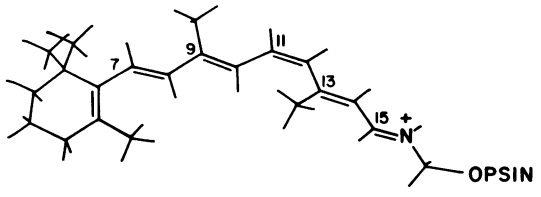

binding to the opsin, protein–chromophore interactions induce an "opsin shift" in the absorption maximum. The absorption maximum ranges from 440 to 580 nm for different opsins, making color vision possible (1). One obvious mechanism for altering the chromophore absorption maximum is protonation of the retinal Schiff base, which shifts the absorption from 370 to 440 nm. Other possible mechanisms include interaction of the chromophore with charged amino acid residues, modulation of the strength of the hydrogen-bonding interaction between the protonated Schiff base moiety and its counterion, and protein-induced changes in chromophore conformation (2).

The mechanisms of the opsin shift in bovine rhodopsin and in bacteriorhodopsin have been extensively characterized. Chemical analogue studies first argued that the 440- to 500-nm opsin shift of the protonated retinal Schiff base absorption in bovine rod visual pigments was due to interaction with a negatively charged amino acid residue near C-13 (3, 4). This idea has been supported by recent solid-state NMR studies of Smith *et al.* (5) and Lugtenburg *et al.* (6). In contrast, ≈3500 cm^{-1} of the 5100-cm^{-1} opsin shift in bacteriorhodopsin arises from a decreased hydrogen-bonding interaction between the protonated Schiff base and its protein counterion (7–9). The additional 1600 cm^{-1} arises from isomerization to a 6-*s-trans* conformation (10, 11) and external charge interactions near C-5 (12, 13).

The factors that dictate the absorption maximum of blue-absorbing visual pigments are unknown. Since the retinal Schiff base absorbs at 370 nm and its protonated form absorbs at 440 nm, a blue-absorbing pigment could contain an unprotonated Schiff base that has its absorption red-shifted by additional interactions with the protein or it may simply contain an unperturbed protonated Schiff base. The study of the opsin shift mechanism in blue-absorbing visual pigments has been hampered by the difficulty of isolating these pigments in quantity and obtaining their spectra. In 1987, Barry and Mathies (14) obtained Raman spectra of the 430-nm bullfrog rod pigment through biochemical isolation and solubilization. Later work examined the solubilized UV-absorbing pigment of the owlfly (15). However, the quality of these data is insufficient to unambiguously characterize the structure of the chromophore and the mechanism of its opsin shift.

These problems can be circumvented by using a laser microprobe to obtain resonance Raman spectra of individual photoreceptor cells (14, 16, 17). In the Raman microprobe, the laser beam illuminates a 5- to 10-μm spot on the sample and the scattered light is analyzed to record the Raman spectrum (18, 19). To study biological samples that are thermally and photochemically unstable, it is necessary to work at low temperature. Therefore, we have developed a 77 K cold stage for our microscope and used it to examine chromophore structure in individual, intact photoreceptors in a variety of species (14, 16, 17). In this paper, we have obtained resonance Raman spectra of the pigment in intact, individual "green rod" (λ_{max} = 440 nm) photoreceptors from the giant marine toad (*Bufo marinus*) and determined the structural factors that dictate the absorption maximum of this blue-absorbing visual pigment. Comparison with resonance Raman data of the bovine 500-nm pigment provides a unique opportunity to examine the mechanism of wavelength regulation in color vision.

The publication costs of this article were defrayed in part by page charge payment. This article must therefore be hereby marked "*advertisement*" in accordance with 18 U.S.C. §1734 solely to indicate this fact.

*Present address: Department of Biochemistry, University of Minnesota, Saint Paul, MN 55108.
†To whom reprint requests should be addressed.

MATERIALS AND METHODS

The design and operation of the Raman microscope have been described (14, 16, 17). Briefly, the photoreceptors are frozen on a specially designed 77 K cold stage (20, 31) and the 4-μm (diameter) probing laser beam is focused onto the 10-μm (diameter) outer segment by the microscope objective (Fig. 1). Raman-scattered light is collected by the objective and dispersed onto a multichannel detector. The spectrograph dispersion and multichannel detector size limit the spectral range to $\approx$700 cm^{-1}. Spectra were calibrated by using an iron hollow-cathode lamp ($\pm$2 cm^{-1}). A buffer and fluorescence background has been subtracted from each spectrum.

The 77 K cold stage consists of a sapphire window mounted on a brass tip that is cooled internally with flowing liquid nitrogen (20, 31). The entire assembly is enclosed in a vacuum chamber fitted with optical windows above and below the sapphire window. The sample-objective (2 mm) and sample-condenser (6 mm) distances maximize thermal isolation without interfering with the operation of the microscope.

Fully dark-adapted retinas from the giant marine toad (*Bufo marinus*) were removed and placed in Ringer's buffer (100 mM NaCl/2.5 mM KCl/1.0 mM $MgCl_2$/5.0 mM $NaHCO_3$/10 mM NaH_2PO_4, pH 7.4). Deuteration of the pigment was accomplished with deuterated Ringer's buffer. The retina was transferred to a drop of Ringer's buffer on the sapphire window of the cold stage, where it was gently teased to remove the photoreceptors and then removed. The sample was covered with a coverslip, and the cold stage was purged with dry, nitrogen gas. After the sample was frozen, the dewar was evacuated and the tip was cooled to 77 K. All procedures were carried out under dim red lights.

At 77 K, laser irradiation produces a steady-state mixture of 11-*cis* rhodopsin, 9-*cis* isorhodopsin, and their common all-*trans* photoproduct, bathorhodopsin. In each case, we have chosen irradiation conditions to give relatively pure spectra of the 9-*cis* form of these pigments. The 9-*cis* form was studied because there are no irradiation conditions that produce pure spectra of the 11-*cis* form at low temperatures (21). Raman spectra of the 9-*cis* form of the green rod pigment were obtained by exciting to the red of the absorption maximum. Scattering from the 9-*cis* form of the green rod pigment predominates with 514.5-nm excitation since both bathorhodopsin and rhodopsin are preferentially pumped to the bluer-absorbing isorhodopsin (21). Spectra of the 9-*cis* form of the toad red rod pigment (λ_{max} = 502 nm) were obtained by pumping at 568 nm to convert the sample to isorhodopsin and probing at 488 nm.

The 9-*cis* protonated Schiff base was made by reacting 1 mg of 9-*cis* retinal with a 10-fold excess of *n*-butylamine in dry ethanol for 30 min. The solvent was evaporated and the resulting Schiff base was redissolved in methanol. The solution was titrated with acidified methanol, concentrated, and placed in a glass capillary cell. Raman spectra were excited with 25 mW of 676-nm light and detected on a photon-counting spectrometer.

RESULTS

Raman spectra of the green rod pigment in H_2O and deuterium-substituted H_2O (D_2O) are presented in Fig. 2. The Raman line at 1662 cm^{-1} is at the expected position for a protonated Schiff base C=NH^+ stretch. The shift of this line to 1636 cm^{-1} in D_2O demonstrates that the blue-absorbing pigment is protonated. Exchange of a proton for a deuteron is expected to shift the C=NH stretch down by $\approx$25 cm^{-1}

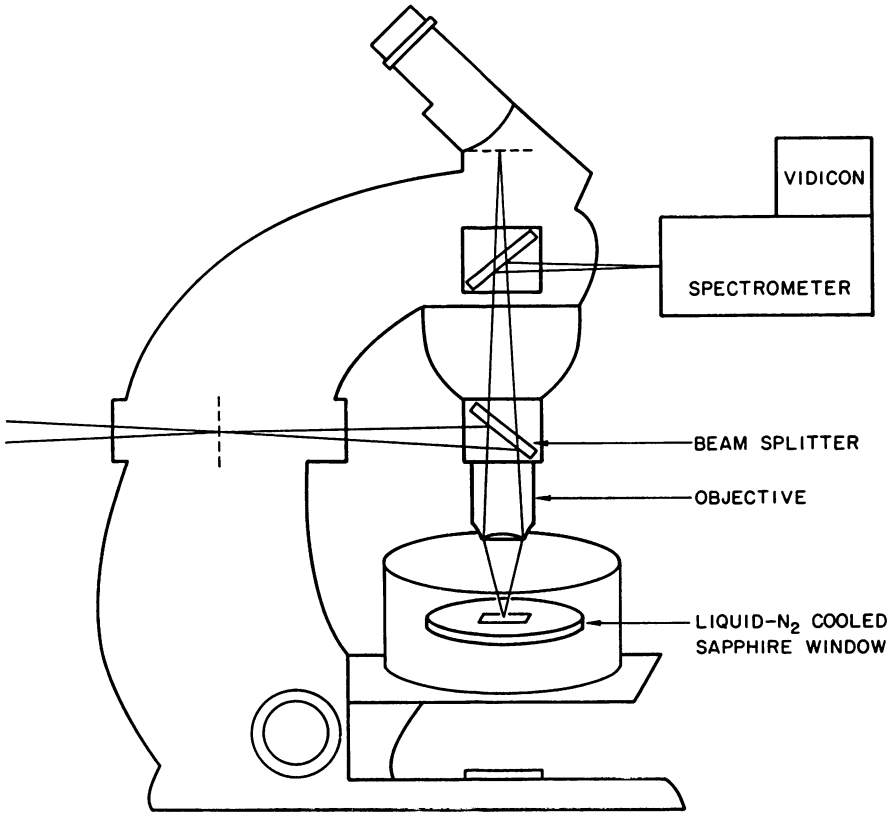

FIG. 1. Raman microscope and liquid nitrogen cold stage. A Zeiss Universal microscope is coupled to a modified Spex 1400 double spectrometer equipped with a cooled, intensified vidicon detector. Long working-length Zeiss LD-epiplan objectives [16×, numerical aperture (n.a.) = 0.3 or 40×, n.a. = 0.6] focus the laser beam on the photoreceptors and collect the Raman scattering.

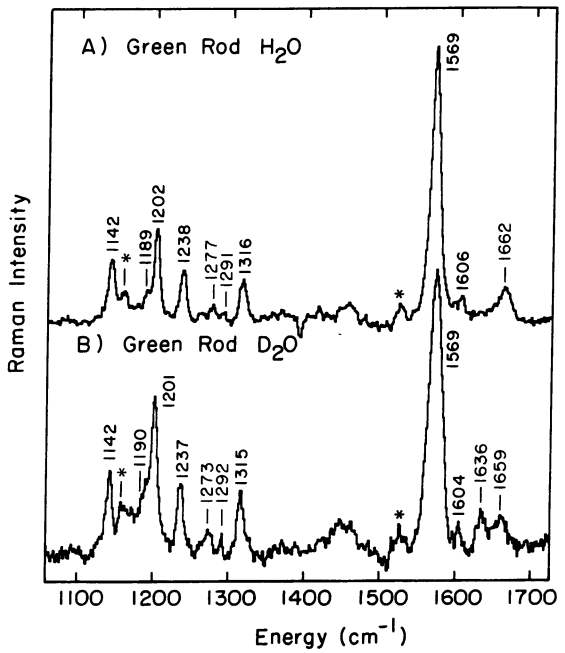

FIG. 2. Resonance Raman microscope spectra of the 9-*cis* isorhodopsin form of the toad green rod pigment in H_2O and D_2O taken with 4.5 mW of 514.5-nm excitation at 77 K. Asterisks indicate lines due to residual carotenoid or bathorhodopsin. Spectra are the sum of four 4-min integrations on each of three or four cells.

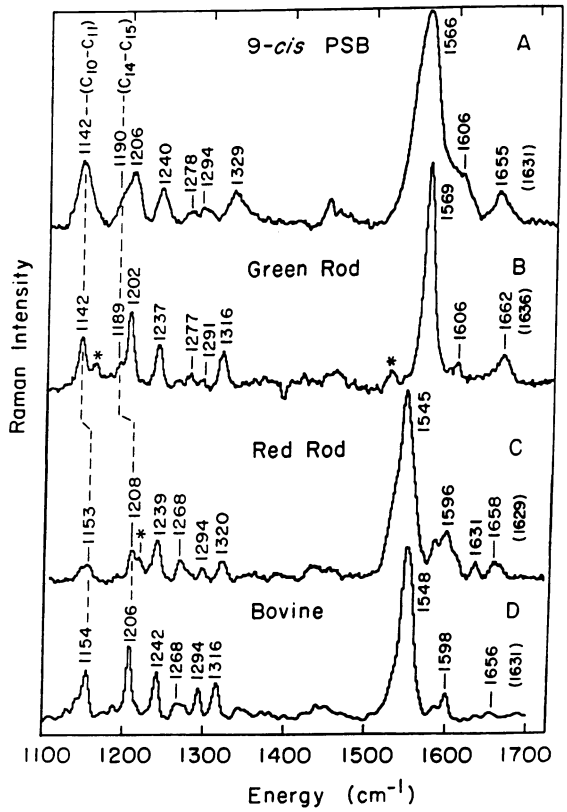

FIG. 3. Comparison of the resonance Raman spectra of the *n*-butylamine 9-*cis* retinal protonated Schiff base (PSB) in methanol (*A*), the toad green rod 9-*cis* pigment (*B*), the toad red rod 9-*cis* pigment (*C*), and the bovine 9-*cis* pigment from Palings *et al.* (25) excited at 568 nm (*D*). The Schiff base frequencies in D_2O are indicated in parentheses. The spectrum in *C* was obtained with a 7.5-mW, 568-nm pump beam and a 4.5-mW, 488-nm probe beam. A methanol spectrum has been subtracted from the spectrum in *A*. Asterisks indicate lines due to residual carotenoid or bathorhodopsin.

because of the increased mass. However, this shift is more correctly explained as being due to the removal of coupling between the N—H rock and the Schiff base stretch (22, 23). The residual intensity at 1659 cm^{-1} in the D_2O spectrum is not completely understood. The relative intensity of this line did not change with D_2O incubation times from 7 to 15 min. Therefore, incomplete H → D exchange is unlikely. Furthermore, red rods in the same field of view were fully exchanged with D_2O, ruling out the possibility of H_2O contamination. The 1659 cm^{-1} feature may be due to the strong amide I band of the opsin protein (24), which is insensitive to deuteration.

Fig. 3 compares Raman spectra of the 9-*cis* retinal *n*-butylamine protonated Schiff base in methanol (λ_{max} = 440 nm), the toad green rod pigment (440 nm), the toad red rod pigment (502 nm), and the bovine isorhodopsin pigment (500 nm). The normal modes in the 1100- to 1300-cm^{-1} fingerprint region of the 9-*cis* protonated Schiff base and bovine isorhodopsin spectra have been assigned through detailed isotopic labeling (25). This work showed that certain modes of the 9-*cis* retinal chromophore exhibit characteristic shifts upon binding to form the 500-nm pigment. The 1142-cm^{-1} C-10–C-11 stretch shifts 12 cm^{-1} to 1154 cm^{-1}, the 1190-cm^{-1} C-14–C-15 stretch shifts 16 cm^{-1} to 1206 cm^{-1}, and the ethylenic band shifts from 1566 to 1548 cm^{-1}. However, neither the C=NH stretching frequency nor the D_2O shift of this mode appears to vary in a systematic way with the absorption maximum. The 1662 cm^{-1} Schiff base frequency in the green rod pigment does suggest that the hydrogen-bonding interaction between the Schiff base moiety and its counterion may be somewhat stronger than that in the red rod and bovine rod pigments. The frequency shifts of the C—C and C=C stretching modes in the bovine pigment are correlated with the presence of a charged residue that perturbs the chromophore near C-13 and shifts the absorption maximum from 440 to 500 nm (3–6). Since the resonance Raman spectra and absorption maxima of the 9-*cis* forms of the bovine and toad red rod pigments are nearly identical, we conclude that the opsin shift of the red rod pigment is also caused by a charge near C-13. In contrast, the frequencies of the C-10–C-11, C-14–C-15, and C=C modes in the green rod pigment are very close to those of the 9-*cis* protonated Schiff base in solution. This indicates that there are no additional protein perturbations acting on the chromophore in the green rod pigment. Although we do not have data on the 11-*cis* form of the green rod pigment, we make the reasonable assumption that it similarly exhibits no protein perturbations other than Schiff base protonation. Thus, the absorption maximum of this blue-absorbing pigment is determined by simple protonation of the Schiff base linkage to the protein that shifts the absorption maximum from ≈370 to 440 nm.

DISCUSSION

Now that the factors that dictate the absorption maximum of blue visual pigments have been defined, the mechanism of wavelength regulation in visual pigments can be discussed in more detail. All known visual pigments have protonated Schiff base chromophores. With no other perturbations, these pigments are expected to absorb near the λ_{max} of the protonated Schiff base in solution (≈440 nm) as found here for the toad green rod. Protein perturbations, most likely charged carboxylate residues, then shift the absorption maximum from 440 to 500 nm in the red rod and bovine pigments (3–6). This perturbation may be a second negatively charged residue in addition to the Schiff base counterion (4), or it may arise from one of the oxygens of the Schiff base anion (26).

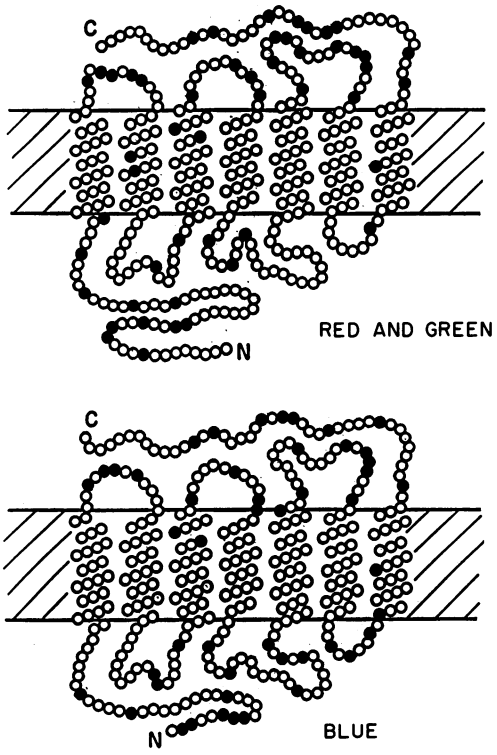

FIG. 4. Comparison of the human blue, green, and red cone opsin amino acid sequences after Nathans *et al.* (29). Charged residues are indicated by filled circles. There is no difference in the number or position of charged intramembrane residues in the red and green opsins. However, two negatively charged residues are lost in the second helix on going from the red/green pigment to the blue pigment.

The recent elucidation of the amino acid sequences of several opsins suggests possible candidates for the protein perturbations that are responsible for the opsin shift in visual pigments (Fig. 4, refs. 27–30, 32). Nathans *et al.* (29, 30) have shown that the negatively charged amino acid residues (Asp-99 and Glu-102) in the human green cone pigment (λ_{max} = 530 nm) are changed to two neutral residues (Gly-80 and Leu-83) in the human blue cone pigment (λ_{max} = 420 nm). They suggested that the removal of these charged residues may be responsible for the difference in opsin shifts of green and blue pigments. Based on the assumption that the toad and human pigment sequences are analogous, our demonstration that a blue pigment contains an *unperturbed* protonated Schiff base with a relatively strong counterion interaction provides experimental support for this hypothesis. When the opsins of the human green and red (λ_{max} = 560 nm) cone pigments are compared, however, no change in the position or number of charged intramembrane residues is found (Fig. 4). This suggests that some mechanism other than alteration of charged amino acid perturbations is responsible for the additional opsin shift in the red cone pigment. Possibilities include changes in the hydrogen-bonding environment near the protonated Schiff base, changes in dipolar residues at other locations in the binding pocket (32), and protein-induced conformational changes of the retinal chromophore as observed in bacteriorhodopsin (7–11). Further Raman microprobe experiments on cone pigments should allow us to examine these possibilities.

We thank Dr. Lubert Stryer for valuable comments and assistance.

This work was supported by a grant from the National Institutes of Health (EY 02051).

1. Lythgoe, J. N. (1972) in *Handbook of Sensory Physiology*, ed. Dartnall, H. J. A. (Springer, New York), Vol. 7/1, pp. 604–624.
2. Kakitani, H., Kakitani, T., Rodman, H. & Honig, B. (1985) *Photochem. Photobiol.* **41**, 471–479.
3. Arnaboldi, M., Motto, M. G., Tsujimoto, K., Balogh-Nair, V. & Nakanishi, K. (1979) *J. Am. Chem. Soc.* **101**, 7082–7084.
4. Honig, B., Dinur, U., Nakanishi, K., Balogh-Nair, V., Gawinowicz, M. A., Arnaboldi, M. & Motto, M. G. (1979) *J. Am. Chem. Soc.* **101**, 7084–7086.
5. Smith, S. O., Palings, I., Copie, V., Raleigh, D. P., Courtin, J., Pardoen, J. A., Lugtenburg, J., Mathies, R. A. & Griffin, R. G. (1987) *Biochemistry* **26**, 1606–1611.
6. Lugtenburg, J., Mathies, R. A., Griffin, R. G. & Herzfeld, J. (1988) *Trends Biochem. Sci.* **13**, 388–393.
7. Harbison, G. S., Herzfeld, J. & Griffin, R. G. (1983) *Biochemistry* **22**, 1–5.
8. Lugtenburg, J., Muradin-Szweykowska, M., Heeremans, C., Pardoen, J. A., Harbison, G. S., Herzfeld, J., Griffin, R. G., Smith, S. O. & Mathies, R. A. (1986) *J. Am. Chem. Soc.* **108**, 3104–3105.
9. Baasov, T. & Sheves, M. (1985) *J. Am. Chem. Soc.* **107**, 7524–7533.
10. Harbison, G. S., Smith, S. O., Pardoen, J. A., Courtin, J. M. L., Lugtenburg, J., Herzfeld, J., Mathies, R. A. & Griffin, R. G. (1985) *Biochemistry* **24**, 6955–6962.
11. van der Steen, R., Biesheuvel, P. L., Mathies, R. A. & Lugtenburg, J. (1986) *J. Am. Chem. Soc.* **108**, 6410–6411.
12. Nakanishi, K., Balogh-Nair, V., Arnaboldi, M. & Tsujimoto, K. (1980) *J. Am. Chem. Soc.* **102**, 7945–7947.
13. Spudich, J. L., McCain, D. A., Nakanishi, K., Okabe, M., Shimizu, N., Rodman, H., Honig, B. & Bogomolni, R. A. (1986) *Biophys. J.* **49**, 479–483.
14. Barry, B. & Mathies, R. A. (1987) *Biochemistry* **26**, 59–64.
15. Pande, C., Deng, H., Rath, P., Callender, R. H. & Schwemer, J. (1987) *Biochemistry* **26**, 7426–7430.
16. Barry, B. & Mathies, R. A. (1982) *J. Cell Biol.* **94**, 479–482.
17. Barry, B., Mathies, R. A., Pardoen, J. A. & Lugtenburg, J. (1987) *Biophys. J.* **52**, 603–610.
18. Abraham, J. L. & Etz, E. S. (1979) *Science* **206**, 716–718.
19. Dhamelincourt, M. C. & Dhamelincourt, P. (1983) *Appl. Spectrosc.* **37**, 512–514.
20. Loppnow, G. R. (1989) Ph.D. Thesis (Univ. of California, Berkeley).
21. Oseroff, A. R. & Callender, R. H. (1974) *Biochemistry* **13**, 4243–4248.
22. Smith, S. O., Myers, A. B., Mathies, R. A., Pardoen, J. A., Winkel, C., van den Berg, E. M. M. & Lugtenburg, J. (1985) *Biophys. J.* **47**, 653–664.
23. Rodman Gilson, H. S., Honig, B. H., Croteau, A., Zarrilli, G. & Nakanishi, K. (1988) *Biophys. J.* **53**, 261–269.
24. Rothschild, K. J., Andrew, J. R., De Grip, W. J. & Stanley, H. E. (1976) *Science* **191**, 1176–1178.
25. Palings, I., Pardoen, J. A., van den Berg, E., Winkel, C., Lugtenburg, J. & Mathies, R. A. (1987) *Biochemistry* **26**, 2544–2556.
26. Birge, R. R., Einterz, C. M., Knapp, H. M. & Murray, L. P. (1988) *Biophys. J.* **53**, 367–385.
27. Ovchinnikov, Y. A. (1982) *FEBS Lett.* **148**, 179–191.
28. Hargrave, P. A., McDowell, J. H., Curtis, D. R., Wang, J. K., Juszczak, E., Fong, S.-L., Rao, J. K. M. & Argos, P. (1983) *Biophys. Struct. Mech.* **9**, 235–244.
29. Nathans, J., Thomas, D. & Hogness, D. S. (1986) *Science* **232**, 193–202.
30. Nathans, J., Piantanida, T. P., Eddy, R. L., Shows, T. B. & Hogness, D. S. (1986) *Science* **232**, 203–210.
31. Loppnow, G. R. & Mathies, R. A. (1989) *Rev. Sci. Instrum.*, in press.
32. Kosower, E. M. (1988) *Proc. Natl. Acad. Sci. USA* **85**, 1076–1080.